CASSINI END-OF-LIFE ESCAPE TRAJECTORIES TO THE OUTER PLANETS*

Masataka Okutsu,† Chit Hong Yam,‡ James M. Longuski,§ and Nathan J. Strange**

We investigate Saturn-escape trajectories via Titan gravity assist as an option for a contamination-free, end-of-life scenario for the Cassini spacecraft. The Saturn-escape energy can be large enough to reach anywhere from the asteroid belt to the Kuiper belt, including the orbital radii of all gas giants, from Jupiter (at 5 AU) to Neptune (at 30 AU). In one example, we present a transfer to Jupiter in which the Cassini spacecraft escapes Saturn in 2012 to impact Jupiter nine years later.

INTRODUCTION

With the Saturn Orbit Insertion (SOI) on July 1, 2004, Cassini-Huygens became the first spacecraft to orbit Saturn.[1] The mission has made a series of exciting discoveries, including finding evidence that Saturn's small satellite Enceladus may harbor water.[2]

The Cassini-Huygens mission has a rich history involving mission design,[3,4] navigation,[5,6] and planetary science.[7,7–9] That history is beyond the scope of this paper; for a brief overview we refer the reader to Yam et al.[10]

Today Cassini continues to explore the Saturnian system. NASA is currently considering a likely two-year extended mission beyond the four-year primary mission, which would take the spacecraft's planned lifetime to at least July 2010. Although Cassini is currently a healthy spacecraft, how the mission may ultimately end is now an important consideration, and the design of the trajectory beyond the summer 2010 will be driven in part by end-of-mission scenarios.

Of primary concern is the possibility that the spacecraft may accidentally impact Enceladus, Titan, or another body and possibly contaminate the local environment. For this reason, the Galileo spacecraft was directed into the Jovian atmosphere upon

* Presented at the AAS/AIAA Astrodynamics Specialist Conference in Mackinac Island, Michigan, August 19–23, 2007.
† Postdoctoral Student, School of Aeronautics and Astronautics, Purdue University, 701 W. Stadium Ave., West Lafayette, Indiana, 47907-2045; Student Member AAS, Student Member AIAA.
‡ Doctoral Candidate, School of Aeronautics and Astronautics, Purdue University, 701 W. Stadium Ave., West Lafayette, Indiana, 47907-2045; Student Member AAS, Student Member AIAA.
§ Professor, School of Aeronautics and Astronautics, Purdue University, 701 W. Stadium Ave., West Lafayette, Indiana, 47907-2045, Member AAS, Associate Fellow AIAA.
** Senior Member of Engineering Staff, Jet Propulsion Laboratory, California Institute of Technology, 4800 Oak Grove Drive, Mail Stop 230-205, Pasadena, California, 91109-8099.

completing its mission in 2003. Likewise, targeting the Cassini spacecraft into Saturn's atmosphere is a possibility.[10] Another option is to place the spacecraft into a "stable orbit" to avoid a collision with any of the moons in the future.[11,12] In this paper, we investigate one such end-of-mission scenario in which the Cassini spacecraft escapes Saturn via gravity assist from Titan to Jupiter, Uranus, or Neptune after many years of heliocentric cruise.

DESIGN STRATEGIES

With its mass two orders of magnitude greater than that of any other Saturnian satellites, Titan is the only gravity-assist body which can significantly change the spacecraft orbit about Saturn. If the period of the final spacecraft orbit is sufficiently large, a Titan flyby enables the spacecraft to escape from Saturn with enough energy to reach perihelion as low as the asteroid belt or aphelion as high as the Kuiper belt.[13] This vast target region includes the orbital radii of the gas giants: Jupiter (at 5 AU), Uranus (at 19 AU), and Neptune (at 30 AU).

Our goal is to design a series of Titan gravity-assists (a tour) that enables a Saturn-escape trajectory to Jupiter, Uranus, or Neptune. We break the design process into the following four steps.

Step 1: Calculate the maximum $v_{\infty/\text{Saturn}}$ that the Cassini can achieve.
Step 2: Find heliocentric trajectories to Jupiter, Uranus, and Neptune.
Step 3: From steps 1 and 2, determine Saturn-escape hyperbolas.
Step 4: Design a series of flybys (a tour) to match $\mathbf{v}_\infty$ for Saturn-escape hyperbolas.

Maximum $\mathbf{V}_\infty$ at Saturn

In Step 1, we determine the maximum $v_{\infty/\text{Saturn}}$ that can be obtained via gravity assist from Titan. Figure 1 shows a vector diagram for a Cassini flyby at Titan, where the spacecraft velocity with respect to Saturn, $\mathbf{v}_o$, is the vector sum of the hyperbolic-excess velocity with respect to Titan, $\mathbf{v}_{\infty/\text{Titan}}$, and Titan's orbital velocity with respect to Saturn, $\mathbf{v}_{\text{Titan}}$. The Titan flyby can change the "pump angle," α, so that the v_o magnitude can increase or decrease while the $v_{\infty/\text{Titan}}$ magnitude remains constant.

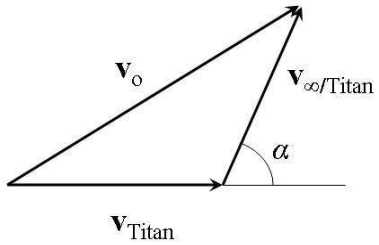

Figure 1 Vector Diagram for the Cassini Spacecraft Flyby at Titan

When $\mathbf{v}_{\infty/\text{Titan}}$ is aligned opposite to $\mathbf{v}_{\text{Titan}}$ (where $\alpha = 180$ deg), $\mathbf{v}_o$ will have its lowest possible value; the Titan encounter occurs at the apoapsis of the spacecraft orbit that has the smallest possible energy for a given $v_{\infty/\text{Titan}}$. On the other hand, when $\mathbf{v}_{\infty/\text{Titan}}$ is aligned to $\mathbf{v}_{\text{Titan}}$ in the same direction (where $\alpha = 0$ deg), the orbital energy is maximum where the Titan encounter occurs at the periapsis of the spacecraft orbit.

Assuming $v_{\infty/\text{Titan}} = 5.9$ km/s (a representative value for Cassini) the spacecraft orbit becomes hyperbolic for $\alpha < 93$ deg, as v_o exceeds the escape speed (from Saturn) of 8.0 km/s. The limiting case on escape energy is the α for the parabolic escape plus the bending angle achieved by the last flyby (7.7 deg for a 1000 km flyby or 7.9 deg for a 900 km flyby). The minimum Titan flyby altitude is 1000 km for the Cassini mission, and we can consider an altitude as low as 900 km for the very last flyby.

For a given flyby altitude, we must increase the period of the final orbit (determined by the pre-flyby α) to increase the Saturn-departure speed (determined by the post-flyby α). Figure 2 shows how Saturn-departure speed increases as the final orbital period increases. We note, however, that costly navigational operations must continue through the final orbit to ensure precise Titan flyby targeting. Although the constraint on the final orbital period is yet to be determined, we use 1 year as a reasonable guideline.

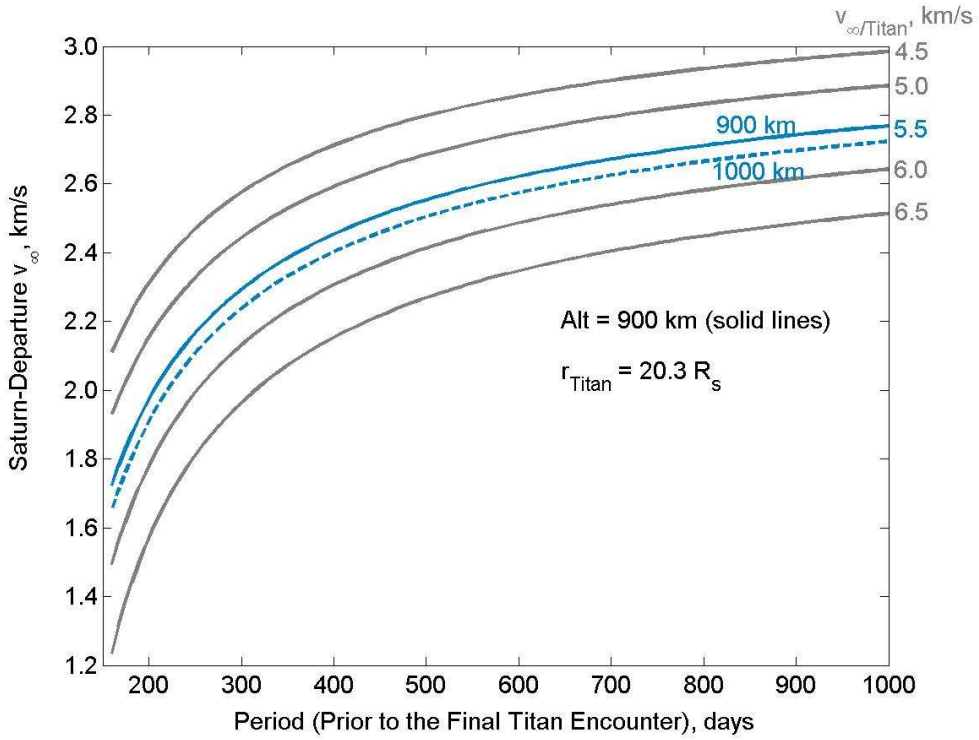

Figure 2 Outgoing v_∞ with Respect to Saturn vs Final Orbital Period about Saturn

We see that a greater $v_{\infty/\text{Saturn}}$ can be achieved when the $v_{\infty/\text{Titan}}$ magnitude is smaller. For $v_{\infty/\text{Titan}}$ = 5.57 km/s, altitude = 900 km, and P = 1 year, the maximum Saturn departure speed is 2.4 km/s.*

In Fig. 2, $v_{\infty/\text{Titan}}$ and P correspond to the values immediately preceding the final flyby; due to the solar perturbations for a large orbit (e.g. P > 100 days) these values are different from those immediately following the penultimate flyby. Figure 3 is a schematic of how solar perturbation moves the Titan encounter location forward from the penultimate flyby to the final flyby. The effects of solar perturbation differ depending on the orientation of the orbit;[14] References 11 and 12 discuss the effects of solar perturbation on large orbits about Saturn in more detail. As an extreme example, if the spacecraft enters a 1500-day orbit (in a certain orientation) via the penultimate flyby, the solar perturbation will be so great that the spacecraft can escape from the Saturnian-system to never return to Titan.[11] For a 1-year-period orbit (that we consider in this paper), solar perturbation can change $v_{\infty/\text{Titan}}$ by hundreds of meters per second.[12] So while we use patched conics throughout most of the analysis in this paper, we incorporate the solar perturbation in the final orbit.

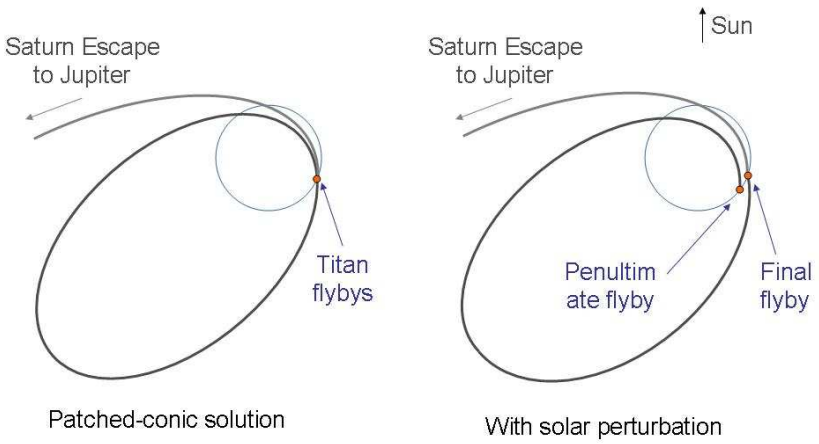

Figure 3 The Final Flyby and the Penultimate Flyby of Titan (Schematic) for Patched-Conic Solution (Left) and Including Solar Perturbation (Right)

Heliocentric Trajectories

In Step 2 we find the Saturn-departure dates that satisfy $v_{\infty/\text{Saturn}}$ < 2.4 km/s as we found in Step 1. Based on our $v_{\infty/\text{Saturn}}$ limit, we see in Fig. 4 that the end of the Cassini

* The $v_{\infty/\text{Saturn}}$ in Fig. 2 is calculated assuming that Titan's orbit is circular. Although Titan's eccentricity of 0.03 causes variations in $v_{\infty/\text{Saturn}}$ (up to ± 58 m/s compared to the circular assumption) depending on the encounter location, this variation is small compared to the magnitude of $v_{\infty/\text{Saturn}}$ (from 1.2 and 3.0 km/s in Fig. 2).

extended mission in July 2010 fortuitously marks the beginning of an injection opportunity to Jupiter, which repeats every 20 years.

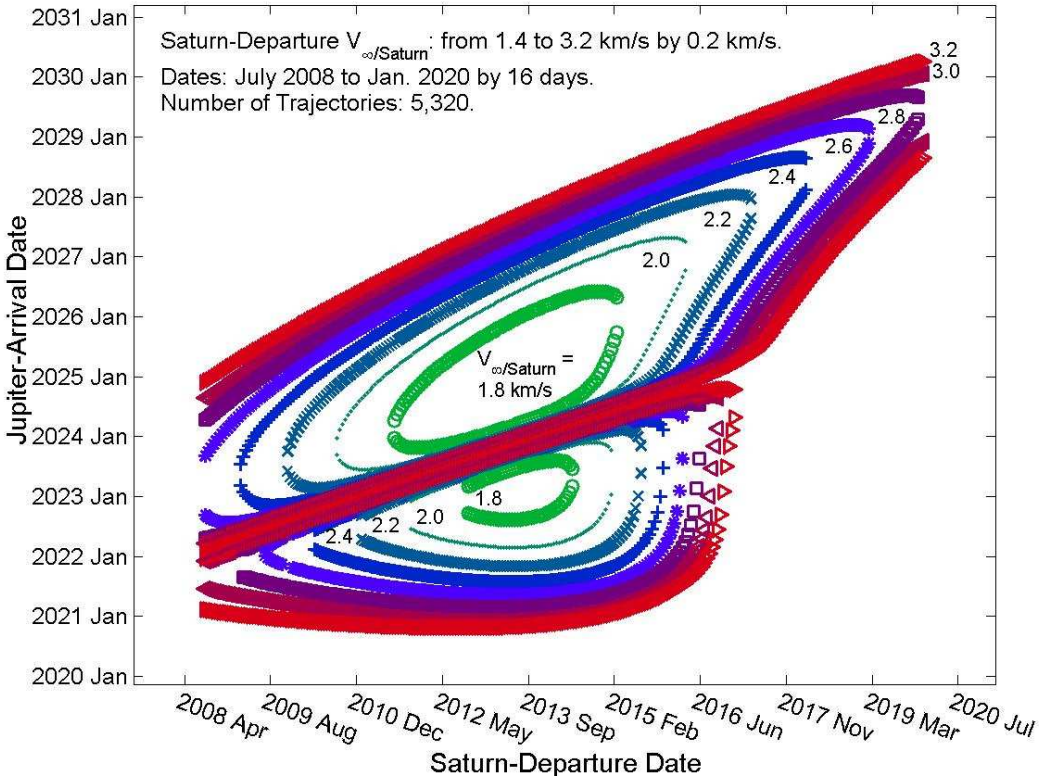

Figure 4 Saturn-to-Jupiter Trajectories (Search Did Not Find Cases for $v_{\infty/\mathrm{Saturn}} \leq 1.6$ km/s)

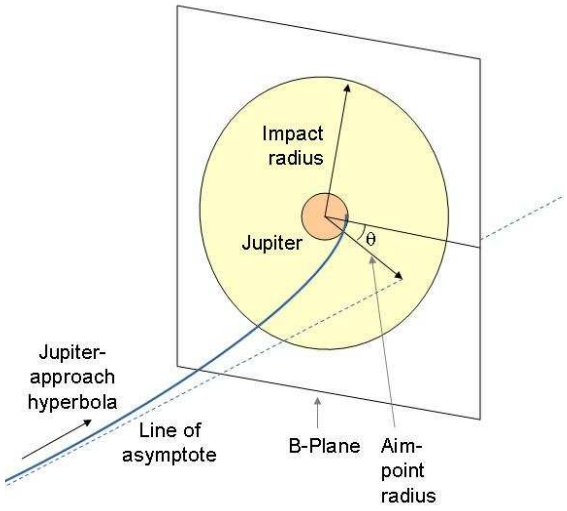

Figure 5 Our Target: Jupiter Impact Radius

In this example, the Cassini mission ends on impact with Jupiter, a seemingly small target when no trajectory correction maneuver is planned (or considered possible) after leaving Saturn. During the heliocentric cruise (which lasts many years), a small initial-velocity error will propagate to a large final-position error. Fortunately, our target, the impact radius, is much greater than Jupiter's radius. As illustrated in Fig. 5, the impact radius is an aim-point radius that guarantees the spacecraft will impact Jupiter.

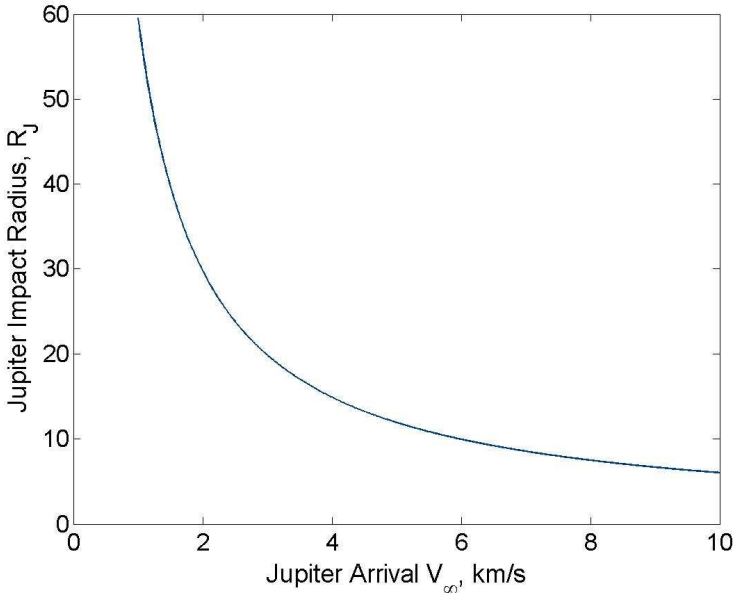

Figure 6 Jupiter Impact Radius vs Jupiter Arrival $\mathbf{v}_\infty$

In Fig. 6, we see that the Jupiter-impact radius increases as the arrival $v_{\infty/\text{Jupiter}}$ decreases. By crudely estimating that an initial velocity error will propagate linearly over the TOF, we find that the allowable initial velocity error for the Saturn-Jupiter transfer is on the order of 4-5 m/s. [For example, in the case of 8.8-year trajectory to Jupiter, $v_{\infty/\text{Jupiter}}$ is 3.9 km/s and the corresponding Jupiter impact radius is 15 R_J (Jovian radii), so that 15 R_J / 8.8 years = 4 m/s.] Because the clean-up maneuvers after the final Titan flyby can reduce the velocity error to less than 10 mm/s, it is well within Cassini's capability to impact Jupiter without any navigation operation after leaving Saturn.[*]

Saturn-Centered Hyperbola

In Step 3, we solve for the Saturn-departure hyperbola that connects the final Titan flyby to the heliocentric trajectory. As we see shortly, there is a range of Titan's

[*] The probability of hitting Europa and other scientifically valuable moons of Jupiter is very small. However, this probability must be calculated and compared to planetary protection requirements before implementing such a scenario. Also we assume that small perturbation forces (such as solar radiation and propellant leakage) have been well calibrated over the duration of the Cassini mission so that their effects can be taken into account with sufficient accuracy.

position within its 16-day orbital period that corresponds to the range of heliocentric trajectories (with different TOF).

Figure 7 is a cross section of the pork-chop plot in Fig. 4 and shows Saturn-to-Jupiter trajectories with various $v_{\infty/Saturn}$ (corresponding to different TOF) that appear in July 2012. As discussed in Step 1, we look for the heliocentric trajectories with $v_{\infty/Saturn} <$ 2.4 km/s (the region below the horizontal line in Fig. 7). We see that the range of TOF that meets our energy criteria is 9.08–10.73 years (for Type I trajectories) and 11.10–13.81 years (for Type II trajectories).

During the 16-day orbital period of Titan, the variations in the Saturn-to-Jupiter trajectories are small (i.e. Fig. 7 looks nearly the same for all departure dates during the 16-day period). However, the Saturn-centered hyperbola is sensitive to Titan's location. Thus we must determine the exact flyby epoch and orbital parameters for the Saturn-centered hyperbola that injects the spacecraft into the heliocentric trajectory.

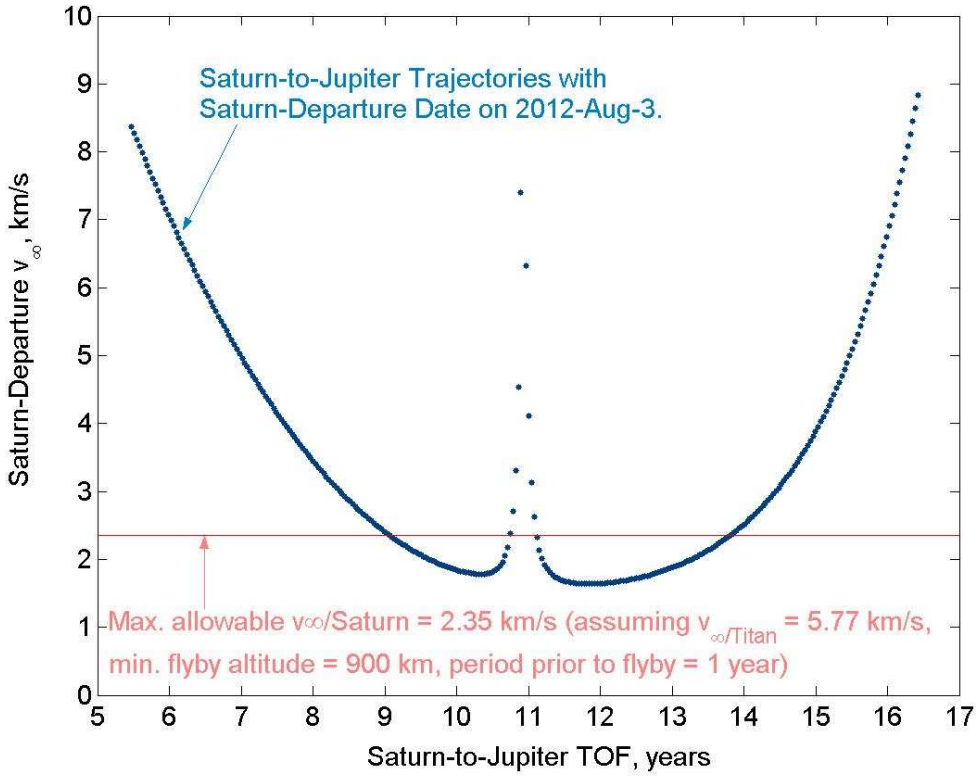

Figure 7 Departure $v_{\infty/Saturn}$ vs. Saturn-Jupiter TOF

We first describe a simple analytical relationship that identifies approximate ranges of Titan flyby locations. Let us first consider a single $\mathbf{v}_{\infty/Saturn}$ vector corresponding to a particular Saturn-to-Jupiter TOF. Assuming that Titan's orbit is circular and is coplanar with Saturn's equatorial plane, then Titan's position can be

expressed by a single variable ϕ, i.e. Titan's angular position measured from the x axis (directed to the first point in Aries). The coordinates are Saturn-Centered Equator Equinox of Epoch. Because Saturn's equator is inclined by 26 deg with respect to the planet's orbital plane, $\mathbf{v}_{\infty/\text{Saturn}}$ often has a large z-component; in the case of the Saturn-to-Jupiter transfer in July 2012, for example, the z-component of $\mathbf{v}_{\infty/\text{Saturn}}$ (which has the overall magnitude of 1.87 km/s) is 0.72 km/s. It can be shown that a hyperbola with sufficiently large inclination must satisfy the following constraint.

$$q = \pm\frac{1}{e^2}\left[\sqrt{e^2-1}\left(\frac{p}{r_o}-1\right) \pm \sqrt{e^2-\left(\frac{p}{r_o}-1\right)^2}\right]\sin(i) - \frac{\mathbf{v}_{\infty/\text{Saturn}}\cdot\hat{\mathbf{z}}}{v_{\infty/\text{Saturn}}} = 0 \tag{1}$$

where

$$p = a\left(1-e^2\right) \tag{2}$$

$$e^2 = 1-\left(2-\frac{r_o}{a}\right)\frac{r_o}{a}\left[\frac{v_T + v_{\infty/\text{Titan}}\cos(\alpha)}{v_o\cos(i)}\right]^2 \tag{3}$$

$$i = \tan^{-1}\left[\frac{\mathbf{v}_{\infty/\text{Saturn}}\cdot\hat{\mathbf{z}}}{\cos(\phi)\mathbf{v}_{\infty/\text{Saturn}}\cdot\hat{\mathbf{y}} - \sin(\phi)\mathbf{v}_{\infty/\text{Saturn}}\cdot\hat{\mathbf{x}}}\right] \tag{4}$$

and where $\mathbf{v}_{\infty/\text{Saturn}}\cdot\hat{\mathbf{x}}$, $\mathbf{v}_{\infty/\text{Saturn}}\cdot\hat{\mathbf{y}}$, and $\mathbf{v}_{\infty/\text{Saturn}}\cdot\hat{\mathbf{z}}$ are x, y, and z components of $\mathbf{v}_{\infty/\text{Saturn}}$. The plus or minus sign outside of the square bracket in Eq. (1) cooresponds to whether $\mathbf{v}_{\infty/\text{Saturn}}$ is outgoing or incoming, respectively. And the plus or minus sign inside of the square bracket corresponds whether the Titan flyby is outbound or inbound, respectively. Because we are describing hyperbolic orbits, the quantity a (corresponding to the semi-major axis for ellipses) is negative and $e > 1$. (We note that a can be computed directly from $v_{\infty/\text{Saturn}}$.) Although not shown here, we can solve for all six orbital elements of the hyperbola from these equations.

As an example, Eq. (1) is plotted in Fig. 8, assuming $\mathbf{v}_{\infty/\text{Saturn}}$ = [-1.45, 0.94, 0.72] km/s, which corresponds to the minimum-energy transfer to Jupiter appearing in late July 2012. We see that no solution exists (i.e. none satisfies the $q = 0$ criterion) if the last Titan flyby were inbound. That is, if the minimum-energy transfer in 2012 were to be used, the final flyby must be outbound at $\phi = 0$ deg.

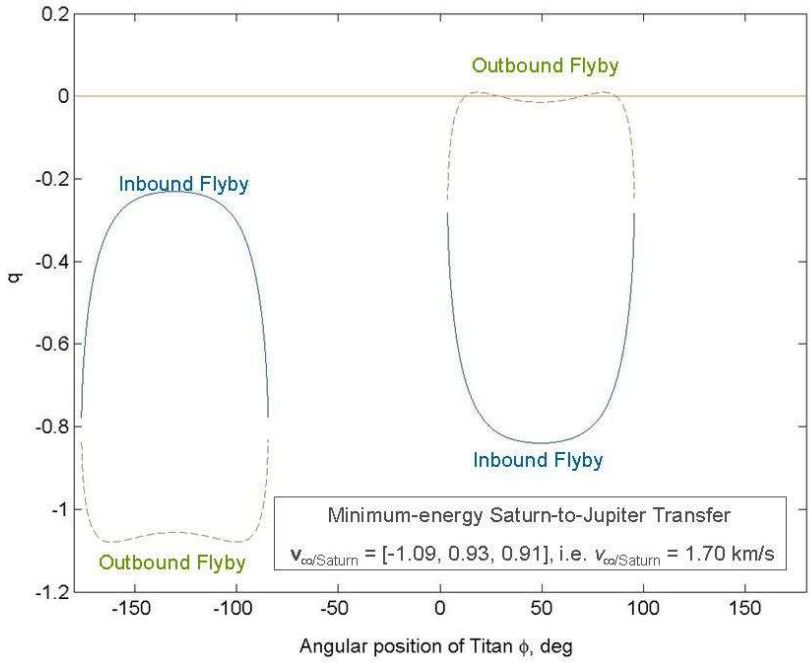

Figure 8 q vs. ϕ for the Saturn-to-Jupiter Minimum-Energy Transfer in July 2013 (Where Solid Lines Indicate Outbound Flybys of Titan and Dashed Indicates Inbound Flybys)

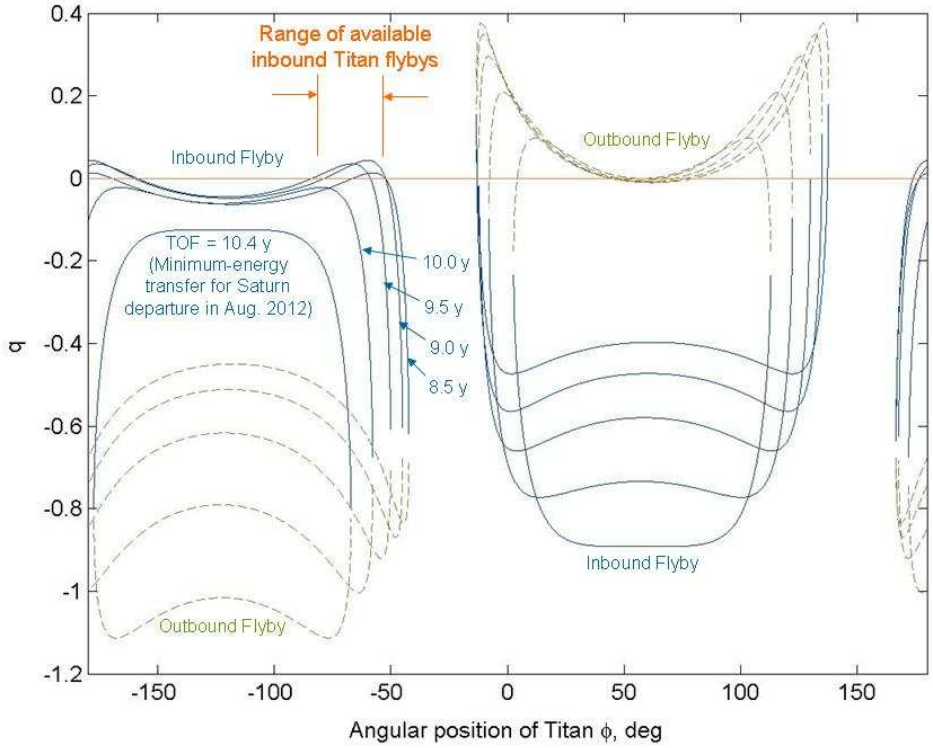

Figure 9 q vs. ϕ for the Saturn-to-Jupiter Transfers in July 2012 (Where TOF Ranging between 7.5 and 9.6 Years)

Likewise, by considering a range of heliocentric trajectories, we identify the range of Saturn-centered hyperbolas that connect to them; it is helpful to have a range (rather than a point) of Titan arrival positions (Fig. 9). We see that inbound flybys becomes feasible (i.e. satisfying $q = 0$) as TOF is decreased to less than 9 years. But the TOF cannot be decreased much further, as Fig. 5 shows that TOF must be above 8 years to satisfy $v_{\infty/Saturn} < 2.4$ km/s. From this analysis, we see that the range of TOF for the heliocentric trajectory is between 8 and 9 years and the corresponding Titan position ϕ is between –90 and –60 deg. That is, as long as the spacecraft performs the final inbound flyby within this 30-deg range of ϕ, the spacecraft can be injected into a heliocentric trajectory to Jupiter with TOF between 8 and 9 years. [For example, a Titan flyby at ϕ = –69 deg (corresponding to July 21, 2013 at 10:16 PM) injects the spacecraft into 8.5-year trajectories to Jupiter.]

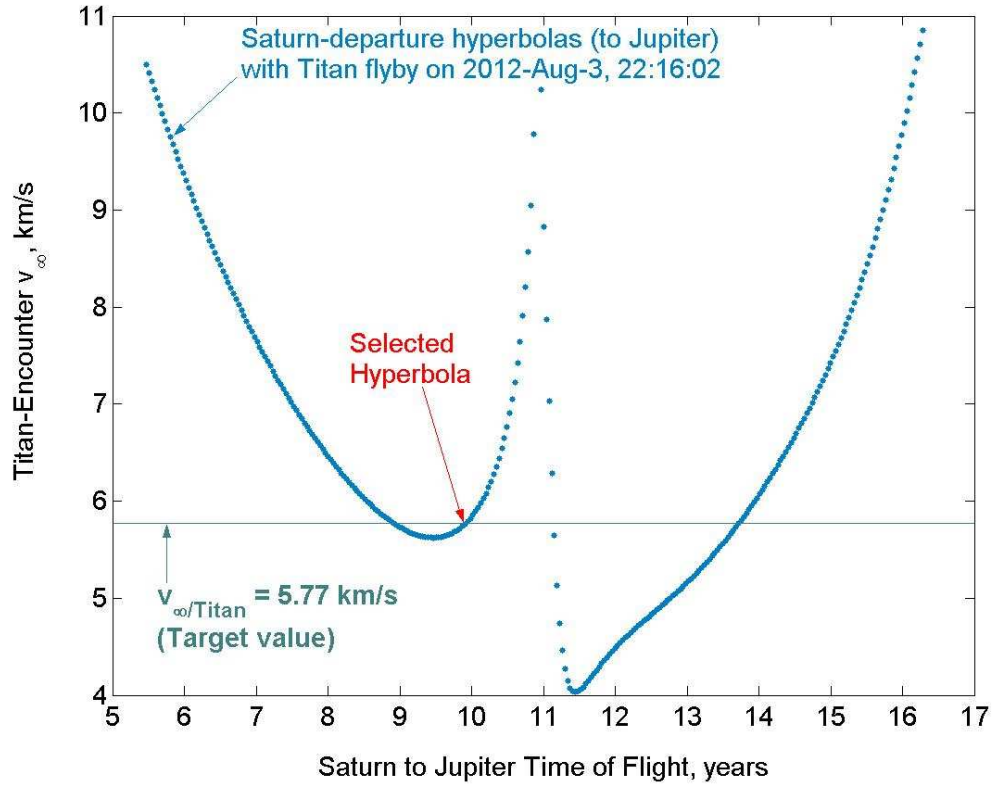

Figure 10 $v_{\infty/Titan}$ vs. Saturn-Jupiter TOF

Although our simple analytical method quickly gives insight into the range of available solutions, a more accurate solution will require an ephemeris for Titan. In Fig. 10, we use Titan's ephemeris model and convert $v_{\infty/Saturn}$ for the heliocentric trajectories (in Fig. 7) into the corresponding $v_{\infty/Titan}$ for the flyby epoch of August 3, 2012 at 22:16:02. As we found from Fig. 5, trajectories with TOF ranges 9.08–10.73 years and

11.10–13.81 years will meet the requirement of $v_{\infty/Saturn} < 2.4$ km/s. We see that there is a heliocentric trajectory with TOF 9.9 years (confirming the prediction of from our simpler analysis in Fig. 9).

While Fig. 9 relates the variation of heliocentric trajectories to Titan's encounter location (i.e. flyby epoch), Fig. 10 relates the variation of heliocentric trajectories to Titan encounter speed at specified flyby epoch. Understanding these bounds is useful. For example, when the Titan flyby occurs on August 3, 2012, the $v_{\infty/Titan}$ of around 5.6 km/s is close to its lower limit for the lower TOF families (Fig. 10). If the $v_{\infty/Titan}$ were reduced to less than 5.6 km/s (via maneuvers or perturbations), longer TOF (of 11.10–13.81 years) must be used.

Flyby Series (Tour) to Match v_∞ for Saturn Escape

In Step 4 we design a tour from the "initial condition" through the last Titan flyby within the range of epoch determined in Step 3. We use a patched-conic propagator known as STOUR, the Satellite Tour Design Program,[15-18] which was originally developed at Jet Propulsion Laboratory (JPL), California Institute of Technology, and was later enhanced at Purdue University. The final few orbits, where solar perturbation is significant, are computed using JPL's CATO.[19] for integration and optimization in a high fidelity gravity model.

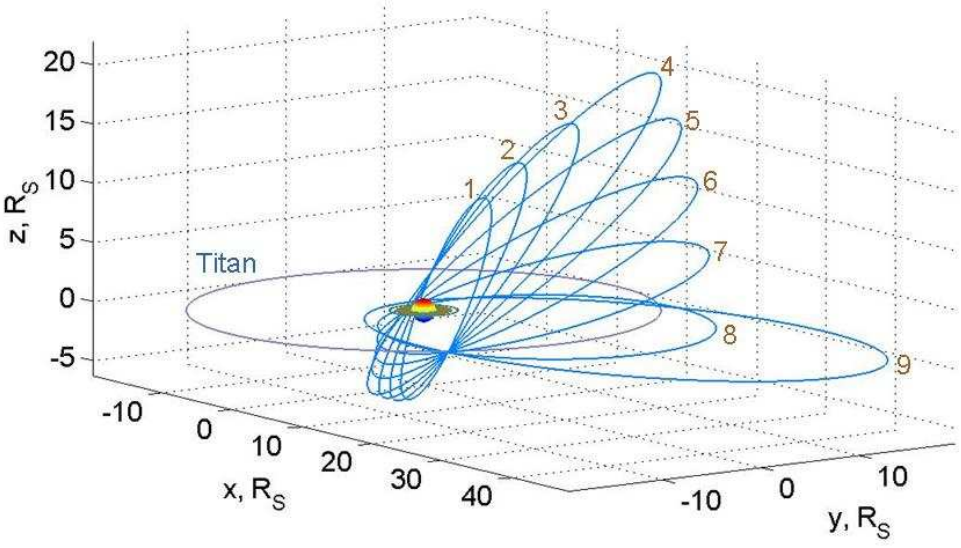

Figure 11 Crank-Down Phase (Coordinates: Saturn-Centered Equator and Equinox of Epoch)

The tour can be broken down to three phases: the crank-down phase, the re-orientation phase, and the pump-up phase. The first phase of the tour is a series of crank downs where we reduce inclination of the spacecraft orbit progressively. Figure 11 shows a trajectory for this phase, where the axes are in Saturnian Radii (i.e. 1 R_S = 60,330 km).

Our end-of-mission sequence begins on July 31, 2008, when a Titan flyby inserts the Cassini spacecraft into an 8-day orbit with periapsis r_p of 3.6 R_S (Saturnian radii) and an inclination i of 69 deg (in the Saturn equatorial frame). This Cassini state corresponds to the one at the end of the primary mission where the $V_{\infty/\text{Titan}}$ is 5.9 km/s. We see in Fig. 11 that nine Titan flybys change the spacecraft orbit from the initial 8-day (1:2 resonance) orbit at 69 deg to the 24-day (3:2 resonance) orbit in the equatorial plane. The TOF for this phase is 239 days. The orbit is labeled according to the number of Titan flybys (instead of the number of orbits) for the end-of-mission scenario.

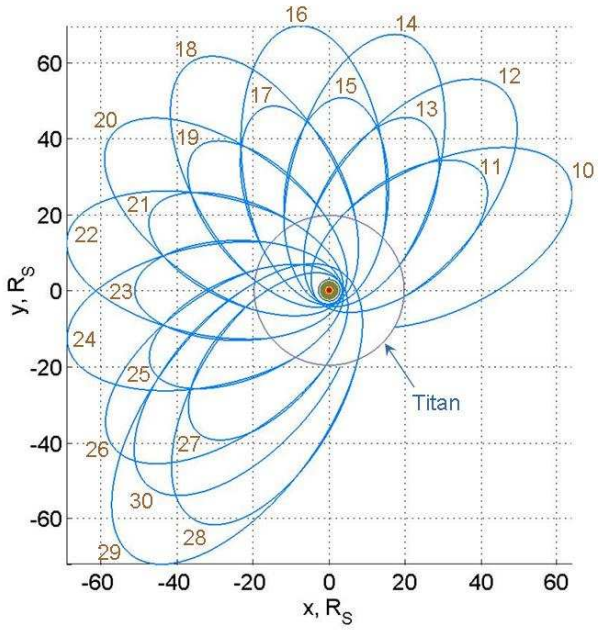

Figure 12 Orbit-Reorientation Phase (Coordinates: Saturn-Centered Equator and Equinox of Epoch)

The line of apsides can be rotated by switching inbound and outbound flybys.[20] If we desire clockwise rotation, we must make either an inbound flyby that increases the spacecraft speed or an outbound flyby that reduces the spacecraft speed. For a counterclockwise rotation, we do the opposite: we combine inbound flybys that reduce the spacecraft speed and outbound flybys that increase the spacecraft speed. Thus by alternating flybys that pump-up (which increase energy) and pump-down (which decreases energy), we can rotate the line of apsides to a desired orientation, at least approximately, in the equatorial plane.

Experience from the Cassini tour design[21-23] shows that alternating 25-day and 40-day orbits is the most efficient way to achieve orbit re-orientation.[22] The tour in Fig. 11 continues in Fig. 12, in which we use the counterclockwise rotation in the equatorial plane. The TOF from Flybys 10–31 is 685 days. We can tune the angle of rotation by using a slightly larger orbit for Flyby 29, to target Flyby 31 to be at the desired location.

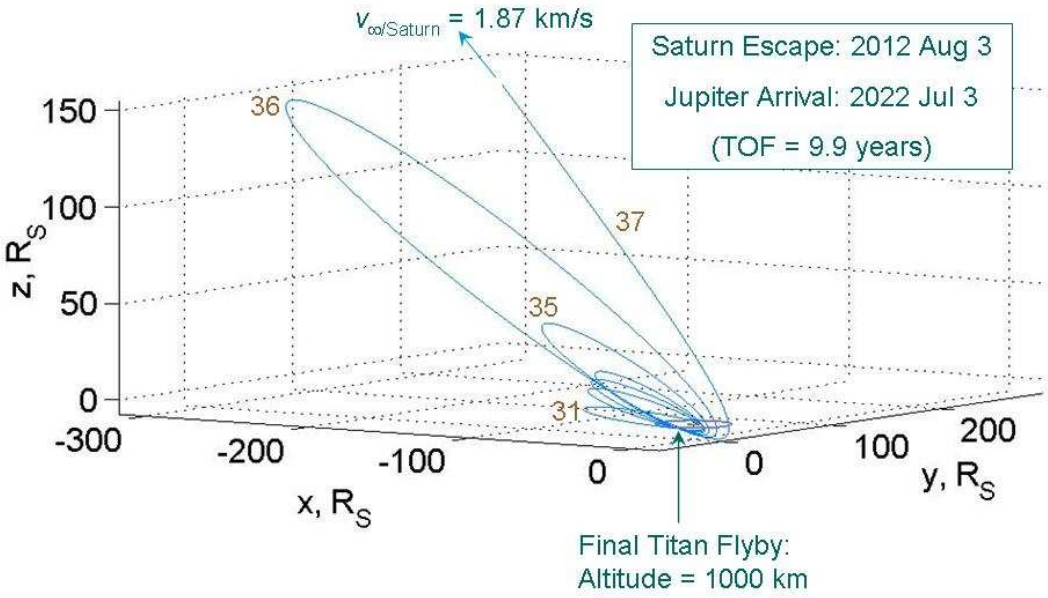

Figure 13 The Final Pump-Up Phase (Coordinates: Saturn-Centered Equator and Equinox of Epoch)

The final phase involves increasing the orbital period up to 1 year (Fig. 13). Because the inclination of Saturn's equator to its orbital plane is large (i.e. 26 deg), $\mathbf{v}_{\infty/Saturn}$ often has a relatively large z-component in the equatorial coordinates. Thus, during this pump-up phase, the orbital inclination must be increased to ensure that the final Titan flyby will be able to produce the desired $\mathbf{v}_{\infty/Saturn}$ vector.

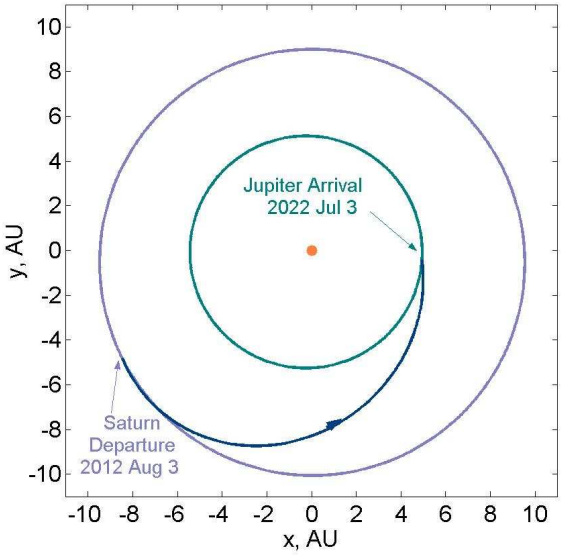

Figure 14 Trajectory Plot of Saturn-to-Jupiter Transfer in July 2012

Table 1
SUMMARY OF TOUR (FROM THE END OF THE PRIMARY MISSION TO SATURN ESCAPE TO JUPITER)[a]

Titan Flyby	Date, yyyy/mm/dd hh:mm	In/Out	Alt., km	θ,[b] deg	V_∞, km/s	P, days	r_p, R_S	i, deg
1	2008/ 7/31 03:19	Out	1000	14	5.89	7.97	3.55	69.2
2	2008/ 8/16 02:01	Out	1000	23	5.89	9.57	4.67	63.2
3	2008/10/ 2 22:05	Out	1000	9	5.91	11.96	5.60	56.9
4	2008/11/19 18:09	Out	1000	1	5.92	15.95	6.52	50.4
5	2008/12/ 5 16:51	Out	1000	-69	5.92	15.95	4.91	44.0
6	2008/12/21 15:32	Out	1000	-75	5.92	15.95	3.68	35.1
7	2009/ 1/ 6 14:13	Out	1000	-81	5.92	15.95	2.86	23.0
8	2009/ 1/22 12:55	Out	1000	-85	5.90	15.95	2.48	8.0
9	2009/ 2/ 7 11:36	Out	1000	-24	5.87	23.92	3.85	1.2
10	2009/ 3/27 07:41	Out	1934	-5	5.84	40.07	5.42	0.4
11	2009/ 5/ 2 20:30	In	2186	0	5.86	24.78	3.94	0.4
12	2009/ 5/31 03:12	Out	2405	0	5.82	40.08	5.30	0.4
13	2009/ 7/ 6 15:54	In	2138	0	5.84	24.79	3.81	0.4
14	2009/ 8/ 3 23:07	Out	2407	0	5.79	40.08	5.15	0.4
15	2009/ 9/ 9 11:41	In	2108	0	5.82	24.80	5.82	0.4
16	2009/10/ 7 19:30	Out	2381	0	5.77	40.09	5.00	0.4
17	2009/11/13 07:53	In	2103	0	5.80	24.80	3.53	0.4
18	2009/12/11 16:19	Out	2333	0	5.75	40.10	4.88	0.4
19	2010/ 1/17 04:33	In	2122	0	5.78	24.81	3.43	0.4
20	2010/ 2/14 13:27	Out	2271	0	5.74	40.10	4.80	0.4
21	2010/ 3/23 01:34	In	2164	0	5.76	24.81	3.38	0.4
22	2010/ 4/20 10:43	Out	2206	0	5.75	40.10	4.78	0.4
23	2010/ 5/26 22:48	In	2223	0	5.74	24.81	3.39	0.4
24	2010/ 6/24 07:55	Out	2151	0	5.76	40.10	4.82	0.4
25	2010/ 7/30 20:02	In	2288	0	5.74	24.81	3.45	0.4
26	2010/ 8/28 04:50	Out	2115	0	5.78	40.09	4.91	0.4
27	2010/10/ 3 17:05	In	2348	0	5.75	24.80	3.56	0.4
28	2010/11/ 1 01:22	Out	2103	0	5.81	40.09	5.04	0.4
29	2010/12/ 7 13:46	In	7795	180	5.77	55.02	5.77	0.4
30	2011/ 2/ 4 03:58	Out	7227	180	5.80	40.08	4.96	0.4
31	2011/ 3/12 16:11	In	1000	-70	5.76	31.89	4.57	12.1
32	2011/ 4/13 13:33	In	1000	-86	5.76	31.89	5.27	23.5
33	2011/ 5/15 10:56	In	4840	-84	5.76	31.89	5.80	28.5
34	2011/ 6/16 08:19	In	4840	-82	5.76	31.89	6.43	32.9
35	2011/ 7/18 04:42	In	1000	-149	5.76	63.79	8.64	32.5
36	2011/ 9/19 23:23	In	1000	-198	5.76	319.97	10.65	26.1
37	2012/ 8/ 4 03:10	In	1000	-147	5.57	—	11.72	28.1

[a]Flybys 1-35 are patched-conic solutions from STOUR which includes no maneuvers. The trajectory from Flyby 35 to Jupiter arrival (which includes a 320-day orbit where solar perturbation is significant) is integrated in CATO; the total ΔV is 38 m/s. The P, r_p, and i for the CATO solutions are values immediately after each apoapsis maneuver.

[b]θ is the angle in the plane perpendicular to the incoming V_∞ vector; where values of 0 and 180 deg correspond (approximately) to equatorial flybys, and –90 and +90 deg correspond (approximately) to flybys over the North and South poles, respectively (Fig. 5).

Because the solar perturbation is significant for the final orbit, Flyby 35 through Jupiter arrival was integrated in CATO. Performing the final Titan flyby on August 4, 2012 at 3:10 AM, the spacecraft escapes Saturn to arrive at Jupiter 9.9 years later in July 2022 (Fig. 14). A summary of the tour is presented in Table 1.

As another example for Saturn escape to Jupiter, Table 2 presents a tour starting from the end of the Cassini Extended Mission (instead of the Primary Mission) in June 2010.* The new tour in Table 2 takes only 2 years (instead of 4 years in Table 1), and the period of the final orbit is only 207 days. The final Titan flyby is now outbound.

Table 2
SUMMARY OF TOUR (FROM THE END OF THE EXTENDED MISSION TO SATURN ESCAPE TO JUPITER)[a]

Titan Flyby	Date, yyyy/mm/dd hh:mm	In/Out	Alt., km	θ,[b] deg	V_∞, km/s	P, days	r_p, R_S	i, deg
1	2010/ 6/21 01:28	Out	1790	8	5.49	23.35	3.99	0.4
2	2010/ 7/10 17:44	In	1850	-180	5.53	39.16	5.74	0.4
3	2010/ 8/22 14:06	Out	2122	-180	5.51	23.36	4.15	0.4
4	2010/ 9/11 07:03	In	1859	-180	5.56	39.17	5.92	0.4
5	2010/10/24 03:19	Out	2150	-180	5.53	23.37	4.34	0.4
6	2010/11/12 20:57	In	1899	-180	5.58	39.17	6.10	0.4
7	2010/12/25 17:08	Out	6613	0	5.56	57.16	7.01	0.4
8	2011/ 2/17 05:21	In	6133	0	5.57	39.18	5.99	0.4
9	2011/ 4/ 1 01:43	Out	1000	138	5.55	23.92	4.59	9.1
10	2011/ 5/18 21:47	Out	1000	152	5.55	15.95	3.35	17.9
11	2011/ 6/ 3 20:29	Out	1000	98	5.55	15.95	4.17	30.6
12	2011/ 6/19 19:10	Out	1000	103	5.55	15.95	5.48	40.1
13	2011/ 7/ 5 17:51	Out	1000	109	5.55	15.95	7.22	46.9
14	2011/ 7/21 16:33	Out	1000	115	5.55	15.95	9.34	51.6
15	2011/ 8/ 6 15:14	Out	1000	123	5.55	15.95	11.78	54.8
16	2011/ 8/22 13:56	Out	1000	133	5.55	15.95	14.47	56.9
17	2011/ 9/ 7 12:37	Out	1000	87	5.55	23.92	17.92	54.0
18	2011/10/25 08:41	Out	1082	68	5.55	47.84	18.89	50.2
19	2011/12/12 04:45	Out	1066	47	5.55	207.29	19.14	46.1
20	2012/ 7/ 6 11:44	Out	1294	22	5.55	–	19.28	42.2

[a]Flybys 1-20 are patched-conic solutions from STOUR which includes no maneuvers.
[b]θ is the angle in the plane perpendicular to the incoming V_∞ vector; where values of 0 and 180 deg correspond (approximately) to equatorial flybys, and –90 and +90 deg correspond (approximately) to flybys over the North and South poles, respectively (Fig. 5).

The planetary-escape technique described in this paper is also applicable (in reverse) to planetary capture, where the spacecraft arriving at Jupiter performs a flyby of one of the moons (e.g. Ganymede) to reduce the spacecraft speed below the escape speed

* As of this writing, the Cassini Extended Mission is proposed, but not officially approved. In this paper, we use representative values for Cassini's state for the proposed Extended Mission.

at Jupiter. References 24–26 present analysis on such satellite-aided capture. Although performing a tour at another planet is an impractical proposal for Cassini, future applications of ballistic capture and escape could open the door to a new class of missions that include nested tours.

SATURN ESCAPE TO URANUS AND NEPTUNE

By following the aforementioned Steps 1-4, we can design tours that permit Saturn-escape trajectories to Uranus and to Neptune. Injection opportunities to these two planets occur during much later dates and the TOF are very long. Furthermore, the weaker (relative to Jupiter) gravities of Uranus and Neptune make their impact radii small, so that the allowable velocity errors at Saturn departure to these two planets are much smaller than the case for Jupiter.

To Uranus

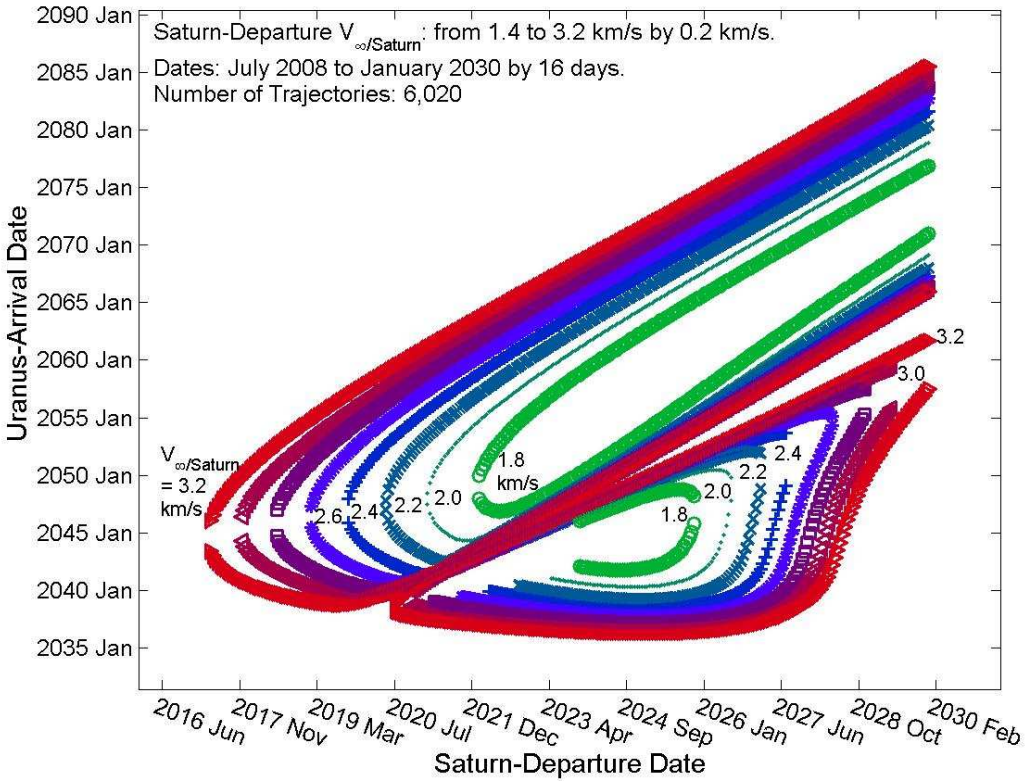

Figure 15 Saturn-to-Uranus Trajectories (Search Did Not Find Cases for $v_{\infty/\text{Saturn}} \leq 1.6$ km/s)

Figure 15 shows Saturn-to-Uranus trajectories. We see that the spacecraft is unable to leave Saturn until 2019 when the required $V_{\infty/\text{Saturn}}$ becomes less than 2.4 km/s as determined in Step 1. To design a Saturnian tour, we choose a slightly later Saturn-departure date of February 2020, so that a range of heliocentric trajectories (rather than a single trajectory) is available when the tour ends.

Table 3
SUMMARY OF TOUR (FROM THE END OF THE EXTENDED MISSION TO SATURN ESCAPE TO URANUS)[a]

Titan Flyby	Date, yyyy/mm/dd hh:mm	In/Out	Alt., km	θ,[b] deg	V_∞, km/s	P, days	r_p, R_S	i, deg
1	2010/ 6/21 01:28	Out	1790	8	5.49	23.35	3.99	0.4
2	2010/ 7/10 17:44	In	1850	-180	5.53	39.16	5.74	0.4
3	2010/ 8/22 14:06	Out	2122	-180	5.51	23.36	4.15	0.4
4	2010/ 9/11 07:03	In	1859	-180	5.56	39.17	5.92	0.4
5	2010/10/24 03:19	Out	2150	-180	5.53	23.37	4.34	0.4
6	2010/11/12 20:57	In	1899	-180	5.58	39.17	6.10	0.4
7	2010/12/25 03:19	Out	2150	-180	5.53	23.37	4.34	0.4
8	2011/ 1/14 11:19	In	1960	180	5.59	39.18	6.22	0.4
9	2011/ 2/26 07:27	Out	1000	24	5.58	111.6	8.38	3.9
10	2011/ 6/17 22:16	Out	1000	91	5.58	111.6	8.81	13.1
11	2011/10/ 7 13:06	Out	1000	92	5.58	111.6	9.69	21.4
12	2012/ 1/27 03:56	Out	1000	94	5.58	111.6	10.95	28.5
13	2012/ 5/17 18:46	Out	1000	95	5.58	111.6	12.49	34.3
14	2012/ 9/ 6 09:36	Out	1000	97	5.58	111.6	14.19	38.8
15	2012/12/27 00:26	Out	1000	99	5.58	111.6	15.91	42.4
16	2013/ 4/17 15:15	Out	1000	102	5.58	111.6	17.48	45.0
17	2013/ 8/ 7 06:05	Out	1000	106	5.57	111.6	18.73	46.7
18	2013/11/26 20:55	Out	1000	-67	5.57	111.6	17.48	45.0
19	2014/ 3/18 11:45	Out	1000	106	5.57	111.6	18.73	46.7
20	2014/ 7/ 8 02:35	Out	1000	-67	5.57	111.6	17.49	45.0
21	2014/10/27 17:25	Out	1000	106	5.57	111.6	18.74	46.7
22	2015/ 2/16 08:15	Out	1000	-67	5.57	111.6	17.49	45.0
23	2015/ 6/ 7 23:04	Out	1000	106	5.57	111.6	18.74	46.7
24	2015/ 9/27 13:54	Out	1000	-67	5.57	111.6	17.50	45.0
25	2016/ 1/17 04:44	Out	1000	106	5.57	111.6	18.74	46.7
26	2016/ 5/ 7 19:34	Out	1000	-67	5.57	111.6	17.50	45.0
27	2016/ 8/27 10:24	Out	1000	106	5.57	111.6	18.75	46.7
28	2016/12/17 01:14	Out	1000	-67	5.57	111.6	17.51	45.0
29	2017/ 4/ 7 16:04	Out	1000	106	5.57	111.6	18.75	46.7
30	2017/ 7/28 06:53	Out	1000	-67	5.57	111.6	17.51	45.0
31	2017/11/16 21:43	Out	1000	106	5.57	111.6	18.76	46.7
32	2018/ 3/ 8 12:33	Out	1000	-67	5.57	111.6	17.52	45.0
33	2018/ 6/28 03:23	Out	1000	106	5.57	111.6	18.76	46.7
34	2018/10/17 18:13	Out	1964	-67	5.57	111.6	17.81	45.4
35	2019/ 2/ 6 09:03	Out	5028	17	5.57	366.7	18.10	43.3
36	2020/ 2/ 8 02:55	Out	1109	21	5.57	—	18.71	39.8

[a]Flybys 1-36 are patched-conic solutions from STOUR which includes no maneuvers.
[b]θ is the angle in the plane perpendicular to the incoming V_∞ vector; where values of 0 and 180 deg correspond (approximately) to equatorial flybys, and –90 and +90 deg correspond (approximately) to flybys over the North and South poles, respectively (Fig. 5).

Table 3 shows a summary of tour that begins with Cassini Extended mission (in June 2010) and ends with Saturn-departure (in February 2020) to reach Uranus 26 years after leaving Saturn. The tour involves 36 flybys, including 27 phasing orbits; while repeating 7:1 resonance orbits (where P = 112 days) the spacecraft waits for 8 years until its departure opportunity to Uranus. Our rough estimate on allowable initial injection error is 0.4 m/s, which is well within the capacity of the Cassini spacecraft.

To Neptune

Heliocentric trajectories to Neptune, located at 30 AU, require high Saturn-departure energy. Even for the minimum-energy trajectory in March 2017 (with TOF to of 44 years), the $V_{\infty/\text{Saturn}}$ is 2.35 km/s (as indicated in Fig. 16) which is near the limit of what can be achieved via gravity assist from Titan. Our tour must end within the small areas in the plot surrounded by the (green) contours of $V_{\infty/\text{Saturn}}$ = 2.4 km/s.

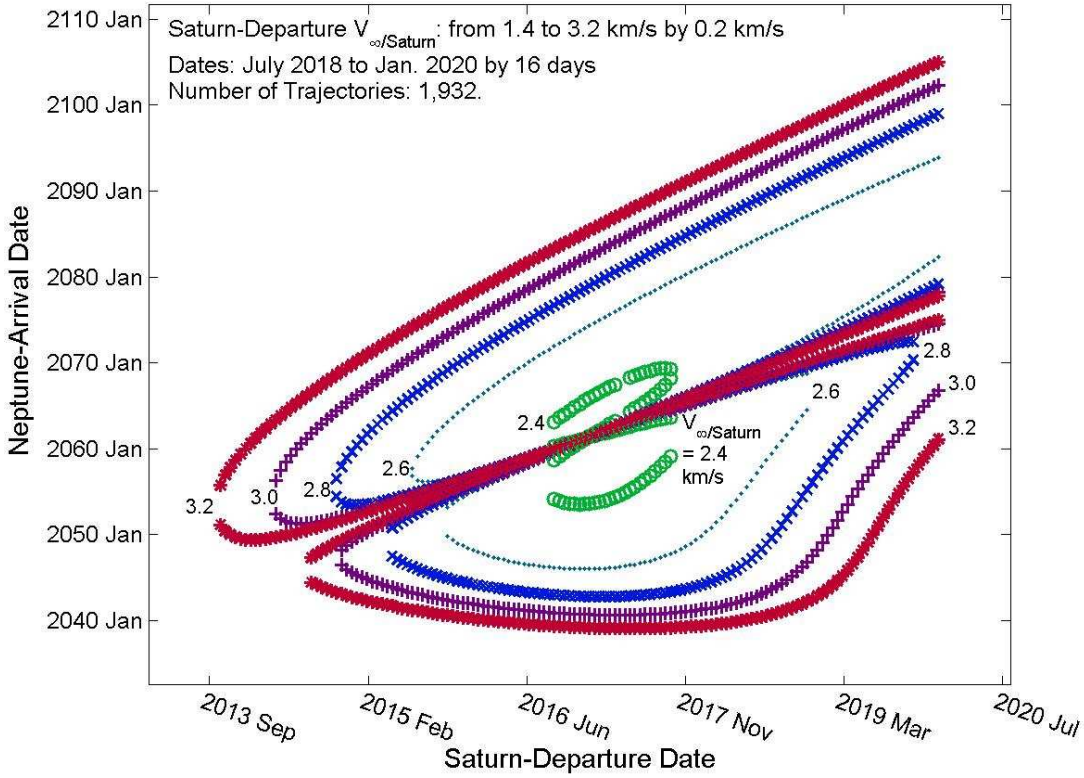

Figure 16 Saturn-to-Neptune Trajectories (Search Did Not Find Cases for $v_{\infty/\text{Saturn}} \leq$ 2.2 km/s)

Table 4 summarizes a tour that ends with a Saturn-escape in March 2017 to reach Neptune 41.3 years later. The tour includes 31 Titan flybys; as in the case to Uranus, many (i.e. 13) phasing orbits with 7:1 resonance are included. The high departure-energy requirement forces the final flyby altitude to be low (at 981 km), but still above the constraint of 900 km. We estimate that the allowable initial velocity error is 0.3 m/s.

Table 4
SUMMARY OF TOUR (FROM THE END OF THE EXTENDED MISSION TO SATURN ESCAPE TO NEPTUNE)[a]

Titan Flyby	Date, yyyy/mm/dd hh:mm	In/Out	Alt., km	θ,[b] deg	V_∞, km/s	P, days	r_p, R_S	i, deg
1	2010/ 6/21 01:28	Out	1790	8	5.49	23.35	3.99	0.4
2	2010/ 7/10 17:44	In	1850	-180	5.53	39.16	5.74	0.4
3	2010/ 8/22 14:06	Out	2122	-180	5.51	23.36	4.15	0.4
4	2010/ 9/11 07:03	In	1859	-180	5.56	39.17	5.92	0.4
5	2010/10/24 03:19	Out	2150	-180	5.53	23.37	4.34	0.4
6	2010/11/12 20:57	In	1899	-180	5.58	39.17	6.10	0.4
7	2010/12/25 17:08	Out	2142	-180	5.56	23.38	4.49	0.4
8	2011/ 1/14 11:19	In	1960	180	5.59	39.18	6.22	0.4
9	2011/ 2/26 07:27	Out	2102	-180	5.58	23.38	4.58	0.4
10	2011/ 3/18 01:55	In	2031	180	5.60	39.18	6.28	0.4
11	2011/ 4/29 22:02	Out	6437	0	5.59	57.15	7.24	0.4
12	2011/ 6/22 10:02	In	6350	0	5.60	39.18	6.26	0.4
13	2011/ 8/ 4 06:10	Out	2075	180	5.59	23.38	4.59	0.4
14	2011/ 8/24 00:40	In	2059	180	5.59	39.18	6.27	0.4
15	2011/10/ 5 20:49	Out	4446	10	5.60	63.78	7.49	0.9
16	2011/12/ 8 15:34	Out	6375	6	5.596	111.62	8.48	1.3
17	2012/ 3/29 06:24	Out	4856	90	5.60	111.62	8.58	6.0
18	2012/ 7/18 21:14	Out	4856	91	5.59	111.62	8.80	10.6
19	2012/11/ 7 12:04	Out	1000	-89	5.59	111.62	8.49	1.3
20	2013/ 2/27 02:54	Out	1000	91	5.59	111.62	8.80	10.6
21	2013/ 6/18 17:44	Out	1000	-89	5.59	111.62	8.49	1.3
22	2013/10/ 8 08:33	Out	1000	91	5.59	111.62	8.81	10.6
23	2014/ 1/27 23:23	Out	1000	-89	5.59	111.62	8.50	1.3
24	2014/ 5/19 14:13	Out	1000	91	5.59	111.62	8.81	10.6
25	2014/ 9/ 8 05:03	Out	1000	-89	5.59	111.62	8.50	1.3
26	2014/12/28 19:53	Out	1000	91	5.59	111.62	8.81	10.6
27	2015/ 4/19 10:43	Out	1000	-89	5.59	111.62	8.51	1.3
28	2015/ 8/ 9 01:32	Out	1000	91	5.59	111.62	8.82	10.6
29	2015/11/28 16:22	Out	1000	-89	5.59	111.62	8.51	1.3
30	2016/ 3/19 07:12	Out	4888	0	5.59	366.74	9.69	1.2
31	2017/ 3/21 01:05	Out	981	0	5.58	—	11.92	1.1

[a]Flybys 1-31 are patched-conic solutions from STOUR which includes no maneuvers.
[b]θ is the angle in the plane perpendicular to the incoming V_∞ vector; where values of 0 and 180 deg correspond (approximately) to equatorial flybys, and –90 and +90 deg correspond (approximately) to flybys over the North and South poles, respectively (Fig. 5).

CONCLUSIONS

We have presented a process in which gravity-assist escape trajectories can be designed to enable the Cassini spacecraft to Jupiter, Uranus, and Neptune. Impact or flyby at Jupiter can be achieved in about 10 years and appears to be well within the capacity of the Cassini spacecraft. Reaching Uranus and Neptune require much longer times of flight (26 years and 44 years, respectively) and involve greater navigation challenges, but appear feasible. A similar approach could be used to target the Cassini spacecraft to other final destinations. Such trajectories provide a technique to end the Cassini mission in such a way to satisfy the planetary quarantine guidelines and at the same time to permit continuing scientific encore investigations before end-of-life impact.

ACKNOWLEDGMENT

This research was funded by the Jet Propulsion Laboratory (JPL), California Institute of Technology, under contract with the National Aeronautics and Space Administration. The research at Purdue University has been supported in part by JPL, under Contract 1283234 (Jeremy B. Jones, Technical Manager). We are grateful to Robert T. Mitchell for his support and to Jeremy B. Jones, John C. Smith, and Brent B. Buffington (all from JPL) and Joseph Gangested and Kevin Kloster (Purdue Graduate Students) for providing useful information, guidance, and helpful suggestions.

NOTATION

a = Semimajor axis of spacecraft orbit (where $a < 0$ for hyperbola), km
e = Eccentricity of spacecraft orbit
i = Inclination of spacecraft orbit, deg
p = Semi-latus rectum (or parameter) of spacecraft orbit, km
P = Period of spacecraft orbit, days
r_o = Spacecraft orbital radius at Titan flyby (i.e. Titan's orbital radius), km
r_p = Periapsis of spacecraft orbit, km
R_J = Equatorial radius of Jupiter, km
R_S = Equatorial radius of Saturn, km
v_o = Spacecraft speed at Titan flyby, km/s
v_{Titan} = Titan's orbital speed, km/s
v_∞ = Hyperbolic excess speed, km/s
α = Pump angle, deg
Δv = Magnitude of a change in velocity, km/s
ϕ = Angular position (i.e. longitude) of Titan in Saturn-centered equatorial coordinates, deg

REFERENCE

1. Goodson, T. D., Buffington, B. B., Hahn, Y., Strange, N. J., Wagner, S. V., and Wong, M. C., "Cassini-Huygens Maneuver Experience: Cruise and Arrival at Saturn," AAS/AIAA Astrodynamics Specialist Conference, Lake Tahoe, CA, AAS Paper 05–286, Aug. 7-11, 2005.

2. Hansen, C. J., Esposito, L., Stewart, A. I. F., Colwell, J., Hendrix, A., Pryor, W., Shemansky, D., West, R., "Enceladus' Water Vapor Plume," *Science*, Vol. 311. No. 5766, March 10, 2006; pp. 1422 – 1425.

3. European Space Agency, "Cassini Saturn Orbiter and Titan Probe, ESA/NASA Assessment Study," ESA REF: SCI(85)1, Aug. 1985.

4. Spilker, L. J. (Editor), *Passage to a Ringed World*, NASA SP-533, Oct. 1997, NASA Special Publication, *http://saturn.jpl.nasa.gov/multimedia/products/product-references.cfm.*

5. Standley, S. P., "Cassini-Huygens Engineering Operations at Saturn," AIAA-2006-5516, SpaceOps 2006 Conference, Rome, Italy, June 19-23, 2006.

6. Wagner, S., Gist, E. M., Goodson, T. D., Hahn, Y., Stumpf, P. W., and Williams, P. N., "Cassini-Huygens Maneuver Experience: Second Year of Saturn Tour," AIAA 2006-6663, AIAA/AAS Astrodynamics Specialist Conference and Exhibit, Keystone, Colorado, Aug. 21-24, 2006.

7. Miner, E. D., "The Cassini-Huygens Mission to Saturn and Titan," Astronomical Data Analysis Software and Systems XI, *ASP Conference Proceedings*, Vol. 281, 2002, pp. 373-381.

8. Matson, D. L., Spilker, L. J., and Lebreton, J.-P., "The Cassini/Huygens Mission to the Saturnian System," *Space Science Reviews*, Vol. 104, No. 1-4 , July, 2002, pp. 1-58.

9. Cuzzi, J. N., Colwell, J. E., Esposito, L. W., Porco, C. C., Murray, C.D., Nicholson, P.D., Spilker, L. J., Marouf, E. A., French, R. C., Rappaport N., and Muhleman, D., "Saturn's Rings: Pre-Cassini Status and Mission Goals," *Space Science Reviews*, Vol. 104, No. 1-4, July, 2002, pp. 209-251.

10. Yam, C. H., Davis, D. C., Longuski, J. M., and Howell, K. C., "Saturn Impact Trajectories for Cassini End-of-Life," AAS/AIAA Astrodynamics Specialists Conference, AAS 07–258, Mackinac Island, Michigan, Aug. 19–23, 2007.

11. Patterson, C., Kakoi, M., Howell, K. C., Yam, C. H., and Longuski, J. M., "500-Year Eccentric Orbits for the Cassini Spacecraft within the Saturn System," AAS/AIAA Astrodynamics Specialists Conference, AAS 07-256, Mackinac Island, Michigan, Aug. 19–23, 2007.

12. Davis, D. C., Patterson, C., and Howell, K. C., "Solar Gravity Perturbations to Facilitate Long-Term Orbits: Application to Cassini," AAS/AIAA Astrodynamics Specialists Conference, AAS 07-275, Mackinac Island, Michigan, Aug. 19–23, 2007.

13. Strange, N.J., "Ballistic Cassini Saturn Escape," JPL Interoffice Memorandum, 343M-2006-001, Jet Propulsion Laboratory, California Institute of Technology, Pasadena, California, March 15, 2006.

14. Yamakawa, H., Kawaguchi, J., Ishii, N., and Matsuo, H., "On Earth-Moon Transfer Trajectory with Gravitational Capture," AAS/AIAA Astrodynamics Specialist Conference, AAS 93-633, Victoria, Canada, 1993.

15. Rinderle, E. A., "Galileo User's Guide, Mission Design System, Satellite Tour Analysis and Design Subsystem," Jet Propulsion Laboratory, California Institute of Technology, Pasadena, CA, JPL D-263, July 1986.

16. Williams, S. N., "Automated Design of Multiple Encounter Gravity-Assist Trajectories," Master's Thesis, School of Aeronautics and Astronautics, Purdue University, West Lafayette, IN, Aug. 1990.

17. Patel, M. R., "Automated Design of Delta-V Gravity-Assist Trajectories for Solar System Exploration," Master's Thesis, School of Aeronautics and Astronautics, Purdue University, West Lafayette, IN, Aug. 1993.

18. Bonfiglio, E. P., "Automated Design of Gravity-Assist and Aerogravity-Assist Trajectories," Master's Thesis, School of Aeronautics and Astronautics, Purdue University, West Lafayette, IN, Aug. 1999.

19. Byrnes, D. V., and Bright, L. E., "Design of High Accuracy Multiple Flyby Trajectories Using Constrained Optimization", *Advances in the Astronautical Sciences*, Vol. 90, Pt. 1, 1995, pp. 121-134.

20. Diehl, R. E., Kaplan, D. I., and Penzo, P. A., "Satellite Tour Design for the Galileo Mission," AIAA Aerospace Sciences Meeting, Reno, Nevada, AIAA Paper 83-0101, Jan. 1983.

21. Wolf, A. A., and Smith, J. C., "Design of the Cassini Tour Trajectories in the Saturnian System," *Control Eng. Practice*, Vol. 3, No. 11, pp. 1611–1619, 1995.

22. Smith, J. C., "Description of Three Candidate Cassini Satellite Tours," AAS/AIAA Astrodynamics Conference, AAS 98-106.

23. Strange, N. J., Goodson, T. D., and Hahn, Y., "Cassini Tour Redesign for the Huygens Mission," AIAA/AAS Astrodynamics Conference, Monterey, California, Aug. 2002.

24. MacDonald, M., and McInnes, C. R., "Spacecraft Planetary Capture Using Gravity-Assist Maneuvers," *Journal of Guidance, Control, and Dynamics*, Vol. 28, No. 2, Mar.-Apr. 2005.

25. Nock, K. T., and Uphoff, C. W., "Satellite Aided Orbit Capture," AAS/AIAA Astrodynamics Specialist Conference, Provincetown, MA, June 1979.

26. Kline, J. K., "Satellite Aided Capture," *Celestial Mechanics*, Vol. 19, pp. 405–415, 1979.

APPENDIX

Derivation of Orbital Elements for Escape/Capture Hyperbolas

Given the outgoing v-infinity vector with respect to the planet (e.g. Saturn), $\mathbf{V}_{\infty/\mathbf{Planet,out}}$, (or the incoming v-infinity vector, $\mathbf{V}_{\infty/\mathbf{Planet,in}}$) and the position vector of the gravity-assist body (e.g. Titan), $\boldsymbol{r}_{ga}$ (= $\boldsymbol{r}_{o}$), we derive expressions for the orbital elements of the escape/capture hyperbola (i.e. a, e, i, Ω, ω, f) and the flyby v-infinity vector with respect to the gravity-assist body (e.g. Titan), $\mathbf{V}_{\infty/\mathbf{ga}}$.

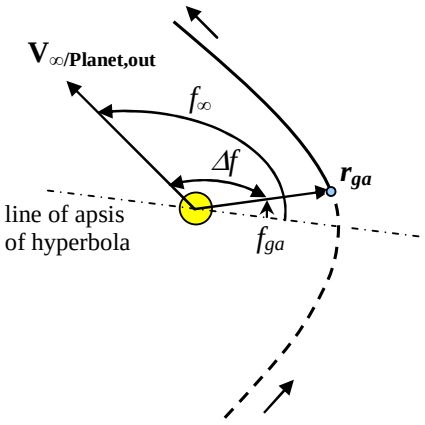

Escape Case 1:

$f_{ga} = f_{\infty} - \Delta f$

$\cos\Delta f = (\mathbf{V}_{\infty}/\|\mathbf{V}_{\infty}\|) \cdot (\boldsymbol{r}_{ga}/\|\boldsymbol{r}_{ga}\|)$

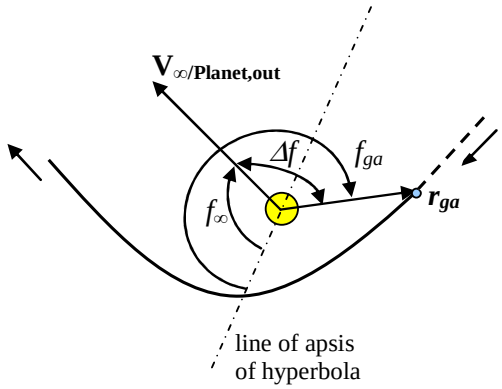

Escape Case 2:

$f_{ga} = f_{\infty} + \Delta f$

$\cos\Delta f = (\mathbf{V}_{\infty}/\|\mathbf{V}_{\infty}\|) \cdot (\boldsymbol{r}_{ga}/\|\boldsymbol{r}_{ga}\|)$

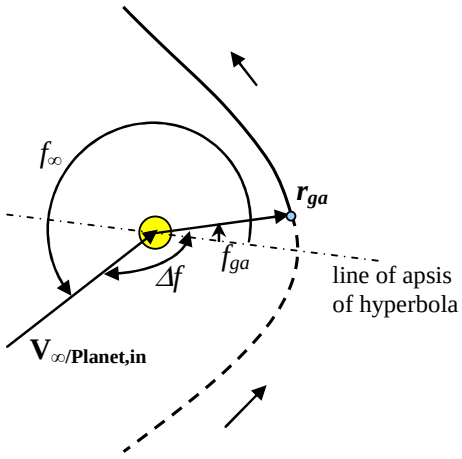

Capture Case 1:

$f_{ga} = (f_{\infty} + \Delta f) - 2\pi$

$\cos\Delta f = -(\mathbf{V}_{\infty}/\|\mathbf{V}_{\infty}\|) \cdot (\boldsymbol{r}_{ga}/\|\boldsymbol{r}_{ga}\|)$

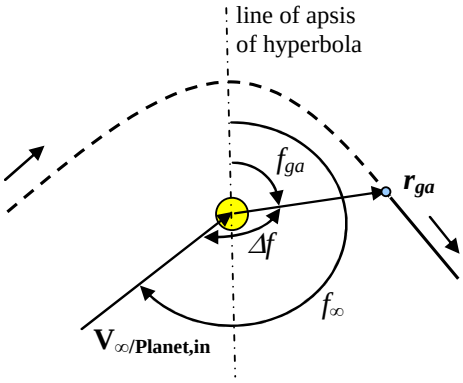

Capture Case 2:

$f_{ga} = f_{\infty} - \Delta f$

$\cos\Delta f = -(\mathbf{V}_{\infty}/\|\mathbf{V}_{\infty}\|) \cdot (\boldsymbol{r}_{ga}/\|\boldsymbol{r}_{ga}\|)$

Figure A-1 Hyperbolic orbits (Planet-centered) for escape (top left and right) and capture (bottom left and right) cases

We note that in Fig. A-1, that f_∞ is the true anomaly of the hyperbolic asymptote, f_{ga} is the true anomaly at encounter of the gravity-assist body, and Δf is the included angle between $\mathbf{V}_\infty$* and $\boldsymbol{r}_{ga}$ for escape cases and $-\mathbf{V}_\infty$* and $\boldsymbol{r}_{ga}$ for capture cases, where $0^o \le \Delta f \le 180^o$.

The semi-major axis of the hyperbola can be found from the magnitude of $\mathbf{V}_\infty$ as

$$a = -\mu / \|\mathbf{V}_\infty\|^2 \tag{A1}$$

From the conic equation

$$r_{ga} = \frac{a(1-e^2)}{1+e\cos f_{ga}} \tag{A2}$$

Rearranging Eq. (A2) gives

$$e^2 + \left(\frac{r_{ga}}{a}\cos f_{ga}\right)e + \left(\frac{r_{ga}}{a} - 1\right) = 0 \tag{A3}$$

To solve Eq. (A3) for the eccentricity e, we need to find an expression for $\cos f_{ga}$ in terms of e and other known quantities. First, we find the true anomaly at infinity as

$$\begin{aligned} f_\infty &= \cos^{-1}(-1/e) \quad \text{for outgoing} \\ &= -\cos^{-1}(-1/e) \quad \text{for incoming} \end{aligned} \tag{A4}$$

Therefore for the escape (outgoing) hyperbola we have

$$\cos f_\infty = -1/e \qquad \sin f_\infty = \sqrt{e^2-1}/e \tag{A5}$$

and for the capture (incoming) hyperbola we have

$$\cos f_\infty = -1/e \qquad \sin f_\infty = -\sqrt{e^2-1}/e \tag{A6}$$

Let $k = \cos\Delta f$, where Δf ($0^o \le \Delta f \le 180^o$) is the difference in true anomaly at infinity and at the encounter location $\boldsymbol{r}_{ga}$ (as mentioned earlier). The cosine and sine of Δf can be computed as

$$\begin{aligned} k = \cos\Delta f &= \mathbf{V}_\infty \cdot \boldsymbol{r}_{ga} / \left(\|\mathbf{V}_\infty\| \cdot \|\boldsymbol{r}_{ga}\|\right) \quad \text{for outgoing} \\ &= -\mathbf{V}_\infty \cdot \boldsymbol{r}_{ga} / \left(\|\mathbf{V}_\infty\| \cdot \|\boldsymbol{r}_{ga}\|\right) \quad \text{for incoming} \end{aligned} \tag{A7}$$

$$\sin\Delta f = \sqrt{1-k^2} \tag{A8}$$

* We refer $\mathbf{V}_{\infty/\text{Planet,out}}$ (for escape) and $\mathbf{V}_{\infty/\text{Planet,in}}$ (for capture) as $\mathbf{V}_\infty$ from now on.

From Fig. A-1, we note that depending on the direction of the orbit, Δf can be defined as $\Delta f = f_{ga} - f_{\infty}$ or $\Delta f = f_{\infty} - f_{ga}$. For an outgoing (escape) hyperbola, we refer to an orbit as "Case 1" when $\Delta f = f_{\infty} - f_{ga}$ and "Case 2" when $\Delta f = f_{ga} - f_{\infty}$. For an incoming (capture) hyperbola, we use "Case 1" when $\Delta f = f_{ga} - f_{\infty} + 2\pi$ and "Case 2" when $\Delta f = f_{\infty} - f_{ga}$.

Using the trigonometric addition formula, the cosine of the true anomaly at $\boldsymbol{r_{ga}}$ can be found as

$$\cos f_{ga} = \cos(f_{\infty} \pm \Delta f) = \cos f_{\infty} \cos \Delta f \mp \sin f_{\infty} \sin \Delta f \tag{A9}$$

Subsitute Eqs. (A5)–(A8) into Eq. (A9) gives

$$\cos f_{ga} = -k/e \pm \sqrt{1-k^2}\sqrt{e^2-1}/e \tag{A10}$$

where the ± sign refers to Case 1 (+ sign) and Case 2 (− sign) orbits, respectively. Subsitute Eq. (A10) into Eq. (A3) obtains

$$e^2 + \tilde{r}\left(-k \pm \sqrt{1-k^2}\sqrt{e^2-1}\right) + (\tilde{r}-1) = 0 \tag{A11}$$

where $\tilde{r} = r_{ga}/a \leq 0$. Simplify and rearrange results in

$$\begin{aligned} e^2 - k\tilde{r} + \tilde{r} - 1 \pm \tilde{r}\sqrt{1-k^2}\sqrt{e^2-1} &= 0 \\ e^2 - \tilde{r}(k-1) - 1 \mp \sqrt{\tilde{r}^2(1-k^2)}\sqrt{e^2-1} &= 0 \end{aligned} \tag{A12}$$

since $\sqrt{\tilde{r}^2} = -\tilde{r}$. Let $A = \tilde{r}^2(1-k^2)$, $B = \tilde{r}(k-1)$, Eq. (A12) becomes

$$e^2 - B - 1 = \pm\sqrt{A}\sqrt{e^2-1} \tag{A13}$$

We note that both A and B are ≥ 0 since the definition of k from Eq. (A7) gurantees that $-1 \leq k \leq 1$. Squaring both sides of Eq. (A13) gives a quadratic equation for e^2:

$$e^4 - (A+2B+2)e^2 + (A+2B+B^2+1) = 0 \tag{A14}$$

Solutions for Eq. (A14) are

$$e_1^2 = (A/2 + B + 1) + \sqrt{A^2/4 + AB} \tag{A15}$$

$$\begin{aligned} e_2^2 &= (A/2 + B + 1) - \sqrt{A^2/4 + AB} \\ &= \left(A + 2B + B^2 + 1\right)/e_1^2 \end{aligned} \tag{A16}$$

where the second expression of Eq. (A16) can have better accuracy (compared with the first expression) in numerical computations. Since $A^2/4 + AB \geq 0$, real solutions for e^2 always exist. We also notice from Eqs. (A15) and (A16) that e_1^2 and $e_2^2 \geq 1$ (i.e. not an ellipse). Subsituting Eqs. (A15) and (A16) back to Eq. (A13), we can confirm that e_1 corresponds to the plus sign and e_2 corresponds to the minus sign of Eq. (A13).

Therefore, for the outgoing (escape) hyperbola we have

$$\text{Case 1: } e = e_1, \quad f_{ga} = \cos^{-1}\left(-1/e_1\right) - \cos^{-1}\left(k\right) \tag{A17}$$

$$\text{Case 2: } e = e_2, \quad f_{ga} = \cos^{-1}\left(-1/e_2\right) + \cos^{-1}\left(k\right) \tag{A18}$$

and for the incoming (capture) hyperbola we obtain

$$\text{Case 1: } e = e_1, \quad f_{ga} = -\cos^{-1}\left(-1/e_1\right) + \cos^{-1}\left(k\right) \tag{A19}$$

$$\text{Case 2: } e = e_2, \quad f_{ga} = -\cos^{-1}\left(-1/e_2\right) - \cos^{-1}\left(k\right) \tag{A20}$$

The solutions from Eqs. (A18) and (A20) are not always physically meaningful as we shall see. We must check the validity of the solutions in Eqs. (A17)–(A20) for the condition of $-f_\infty \leq f_{ga} \leq f_\infty$, or

$$\cos f_{ga} \geq \cos f_\infty = -1/e \tag{A21}$$

Subsitution of Eq. (A10) into Eq. (A21) yields the condition for a valid solution of e:

$$\left(1-k\right) \pm \sqrt{1-k^2}\sqrt{e^2-1} \geq 0 \tag{A22}$$

Since $-1 \leq k \leq 1$, Case 1 ($e = e_1$) solutions always satisfy Eq. (A22) while Case 2 solutions may or may not satisfy Eq. (A22) (depending on the value of $\tilde{r}$ and k).

From $\mathbf{V}_\infty$ and $\boldsymbol{r}_{ga}$, the direction of the angular momentum vector (which defines the direction of the orbital motion) can be found as

$$\text{Outgoing Case 1: } \hat{h} = \boldsymbol{r}_{ga} \times \mathbf{V}_\infty \Big/ \left\| \boldsymbol{r}_{ga} \times \mathbf{V}_\infty \right\| \tag{A23}$$

$$\text{Outgoing Case 2: } \hat{h} = \mathbf{V}_\infty \times \boldsymbol{r}_{ga} \Big/ \left\| \mathbf{V}_\infty \times \boldsymbol{r}_{ga} \right\| \tag{A24}$$

$$\text{Incoming Case 1: } \hat{h} = \left(-\mathbf{V}_\infty\right) \times \boldsymbol{r}_{ga} \Big/ \left\| \left(-\mathbf{V}_\infty\right) \times \boldsymbol{r}_{ga} \right\| = \boldsymbol{r}_{ga} \times \mathbf{V}_\infty \Big/ \left\| \boldsymbol{r}_{ga} \times \mathbf{V}_\infty \right\| \tag{A25}$$

$$\text{Incoming Case 2: } \hat{h} = \boldsymbol{r}_{ga} \times \left(-\mathbf{V}_\infty\right) \Big/ \left\| \boldsymbol{r}_{ga} \times \left(-\mathbf{V}_\infty\right) \right\| = \mathbf{V}_\infty \times \boldsymbol{r}_{ga} \Big/ \left\| \mathbf{V}_\infty \times \boldsymbol{r}_{ga} \right\| \tag{A26}$$

where $\hat{h}$ is the unit vector of the angular momentum. From $\hat{h}$ and $\hat{r}$ (the unit vector of $\boldsymbol{r}_{ga}$), we can determine the orbital elements i, Ω, and ω as follows:

$$\hat{r} = \boldsymbol{r}_{ga} \Big/ \left\| \boldsymbol{r}_{ga} \right\| \tag{A27}$$

$$\hat{\theta} = \hat{h} \times \hat{r} \tag{A28}$$

$$\cos i = \hat{h}_z \tag{A29}$$

$$\sin \Omega = \hat{h}_x \big/ \sin i \,, \qquad \cos \Omega = -\hat{h}_y \big/ \sin i \tag{A30}$$

$$\sin \theta = \hat{r}_z \big/ \sin i \,, \qquad \cos \theta = \hat{\theta}_z \big/ \sin i \tag{A31}$$

$$\omega = \theta - f_{ga} \tag{A32}$$

where $\hat{h}_x, \hat{h}_y, \hat{h}_z$ are the $\hat{x}, \hat{y}, \hat{z}$ components of $\hat{h}$; $\hat{r}_z, \hat{\theta}_z$ are the $\hat{z}$ components of $\hat{r}$ and $\hat{\theta}$, respectively. For the special case of equatorial orbit (i.e. i = 0° or 180°), Ω is set to an arbitrary value (e.g. 0°) and the angle θ is computed from

$$\sin\left(\Omega + \theta\right) = \hat{r}_y \qquad \cos\left(\Omega + \theta\right) = \hat{r}_x \qquad \text{when } i = 0^{\circ} \tag{A33}$$

$$\sin\left(\Omega - \theta\right) = \hat{r}_y \qquad \cos\left(\Omega - \theta\right) = \hat{r}_x \qquad \text{when } i = 180^{\circ} \tag{A34}$$

The velocity of the spacecraft (with respect to the central body), $\mathbf{V_{sc}}$, can be computed from the orbital elements of the hyperbolas as

$$\mathbf{V_{sc}} = \left[\mu e \sin f_{ga} \Big/ \sqrt{\mu a (1 - e^2)} \right] \hat{r} + \left[\mu \left(1 + e \cos f_{ga} \right) \Big/ \sqrt{\mu a (1 - e^2)} \right] \hat{\theta} \tag{A35}$$

The flyby v-infinity vector with respect to the gravity-assist body (e.g. Titan), $\mathbf{V_{\infty/ga}}$, can be calculated from

$$\mathbf{V_{\infty/ga}} = \mathbf{V_{sc}} - \mathbf{V_{ga}} \tag{A36}$$

where $\mathbf{V_{ga}}$ is the velocity of the gravity-assist body (relative to the central body). For a feasible flyby (at the gravity-assist body), the magnitude of $\mathbf{V_{\infty/ga}}$ computed from Eq. (A36) should match with the incoming $\|\mathbf{V_{\infty/ga}}\|$ (e.g. for the Cassini spacecraft, $\|\mathbf{V_{\infty/Titan}}\|$ is around 5.50 km/s).